

See discussions, stats, and author profiles for this publication at: <https://www.researchgate.net/publication/276285842>

Anti-Inflammatory Sesquiterpenes from the Medicinal Herb *Tanacetum sinaicum*

Article in RSC Advances · May 2015

DOI: 10.1039/C5RA07511

CITATIONS

2

READS

3,326

7 authors, including:



Mohamed Elamir F. Hegazy

National Research Center, Egypt

168 PUBLICATIONS 1,469 CITATIONS

[SEE PROFILE](#)



Ahmed Ragab Hamed

National Research Center, Egypt

63 PUBLICATIONS 323 CITATIONS

[SEE PROFILE](#)



Tarik Mohamed

National Research Center, Egypt

61 PUBLICATIONS 463 CITATIONS

[SEE PROFILE](#)



Paul Pare

Texas Tech University

184 PUBLICATIONS 10,747 CITATIONS

[SEE PROFILE](#)

Some of the authors of this publication are also working on these related projects:

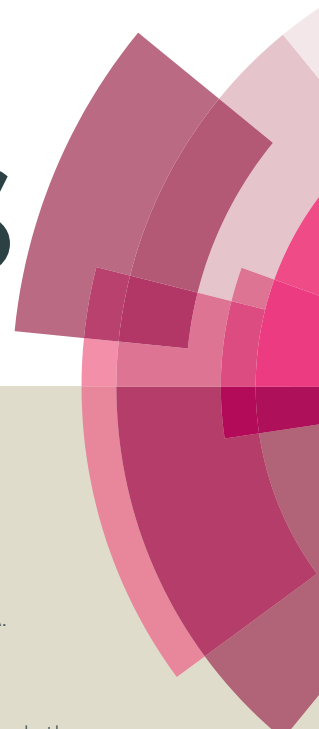


write paper [View project](#)



Hi, we study each other. [View project](#)

RSC Advances



This article can be cited before page numbers have been issued, to do this please use: M. E. Hegazy, A. R. Hamed, T. A. Mohamed, A. Debbab, S. Nakamura, H. matsuda and P. W. Pare, *RSC Adv.*, 2015, DOI: 10.1039/C5RA07511D.



This is an *Accepted Manuscript*, which has been through the Royal Society of Chemistry peer review process and has been accepted for publication.

Accepted Manuscripts are published online shortly after acceptance, before technical editing, formatting and proof reading. Using this free service, authors can make their results available to the community, in citable form, before we publish the edited article. This *Accepted Manuscript* will be replaced by the edited, formatted and paginated article as soon as this is available.

You can find more information about *Accepted Manuscripts* in the [Information for Authors](#).

Please note that technical editing may introduce minor changes to the text and/or graphics, which may alter content. The journal's standard [Terms & Conditions](#) and the [Ethical guidelines](#) still apply. In no event shall the Royal Society of Chemistry be held responsible for any errors or omissions in this *Accepted Manuscript* or any consequences arising from the use of any information it contains.



Anti-Inflammatory Sesquiterpenes from the Medicinal Herb *Tanacetum sinaicum*

Mohamed-Elamir F. Hegazy,^a Ahmed R. Hamed,^a Tarik A. Mohamed,^a Abdessamad Debbab,^b Seikou Nakamura,^c Hisashi Matsuda^c and Paul W. Paré^d

Received 00th January 20xx,
Accepted 00th January 20xx

DOI: 10.1039/x0xx00000x

www.rsc.org/

New sesquiterpenes tanacetolide A-C (**1-3**) were isolated from a *Tanacetum sinaicum* extract together with known compounds (**4-10**). Structures were elucidated on the basis of MS and NMR spectroscopic data. All compounds were evaluated for the inhibition of inducible nitric oxide (NO) production in a mouse peritoneal macrophage system. Iso-seco-tanaparholide-3-O-methyl ether (**4**) produced potent inhibition of NO production (IC₅₀ = 1.0 μM). At the protein expression level, **4** elicited concentration-dependant down-regulation of inducible nitric oxide synthase.

Introduction

Sesquiterpene lactones and flavonoids, in addition to functioning as taxonomic traits for plant systematists in the genus *Tanacetum*,^{1,2} can also function as anti-inflammatory agents. The genus *Tanacetum* comprises approximately 150 species located throughout Europe and Asia from the Mediterranean to Iran with many plants in the genus having been investigated for their traditional uses in medicine.^{3,4} *Tanacetum sinaicum* is indigenous to the Middle East and for this study was collected from Saint Katherine Protectorate, a sheltered area in the Sinai (Egypt) due to wildlife diversity and ecosystem complexity. Traditional uses for *T. sinaicum* (also known as *T. santolinoides*, *Santolina sinaica* or *Pyrethrum santolinoides*)⁵ include treatment of fevers, migraines, stomach ailments, bronchitis and arthritis.^{3,4} The scope of this phytochemical investigation is to chemically characterize metabolites containing anti-inflammatory activity and examine their mode of action.

Chronic inflammatory diseases such as rheumatoid arthritis and asthma are associated with upregulation of nitric oxide (NO).⁶ While NO plays an important role in tissue homeostasis, it also has been implicated in pathological conditions including inflammation. NO is produced by nitric oxide synthase (NOS) as a by-product during the reaction converting L-arginine to L-citrulline.⁷ Constitutive forms include endothelial (eNOS) and neuronal (nNOS) isoforms that are

expressed in vascular endothelial and nervous system cells, respectively. While these forms rapidly generate small amounts of NO to mediate homeostatic regulations such as vasodilation and platelet fluidity, an inducible isoform, iNOS produces relatively high NO levels in response to pathogen infection; with defense responses, NO emissions result in localized cell death. iNOS expression is activated by at least three signaling pathways including the mitogen protein kinase family (MAPKs) that phosphorylates the transcription factors p38, ERK and JNK, the nuclear factor NF-κB and signal transducers and activators of transcription (STAT1).⁸⁻¹¹

Since iNOS can exacerbate inflammatory diseases, it is currently considered a good target for the alleviation or treatment of chronic inflammation.¹⁰ Herein is reported the extraction, isolation and structure elucidation of natural products from *T. sinaicum* as well as biological activity as anti-inflammatory agents using a NO production assay.

Results and discussion

Chromatographic fractionation and purification of an organic extract of *T. sinaicum* afforded three new metabolites in addition to known compounds iso-seco-tanaparholide-3-O-methyl ether (**4**),¹² 11,13-dihydroridentin (**5**),¹³ 1α,3-β-dihydroxy-7-α,11-β-H-germacra-4Z,10(14)-dien-12,6-α-olide (**6**),¹⁴ arsanin (**7**),¹⁵ 1-α,3-β-dihydroxy-7-α,11-β-H-germacra-4Z,9Z-dien-12,6α-olide (**8**),¹⁶ ketopelenolide B (**9**)¹⁴ and 3-β-hydroxy-11(αH),13-dihydrocostunolide (**10**)¹⁷ (Fig. 1).

Compound **1** was obtained as colorless oil with an optical rotation of $[\alpha]_D^{25} +55.6$ in MeOH. HRFABMS analysis showed a molecular ion peak at m/z 267.1590 $[M-OOH]^+$ (calcd. for C₁₅H₂₃O₄, 267.1596), corresponding to the molecular formula of C₁₅H₂₄O₆. The IR spectrum showed characteristic bands at 3450 cm⁻¹ (OH) and 1695 cm⁻¹ (CO). ¹H-NMR showed methyl signals at δ_H 0.94 (s), 1.19 (d, $J = 6.8$), and 1.39 (s), three oxygenated methine signals at δ_H 3.12 (brs), 3.69 ($J = 5.5, 10.4$) and an additional downfield signal at δ_H 3.95 (t, $J = 11.0$) (Table 1). ¹³C NMR and DEPT established the

^a Phytochemistry Dept/Center Excellence for Advanced Sciences, National Research Centre, 33 El Bohouth St Dokki, Giza, Egypt, P. O. 12622.

^b Pharmaceutical Institut für Pharmazeutische Biologie und Biotechnologie, Heinrich-Heine-Universität Düsseldorf, D-40225 Düsseldorf, Germany.

^c Kyoto Pharmaceutical University, Yamashina-ku, Kyoto 607-8412, Japan.

^d Dept of Chemistry & Biochemistry Texas Tech University, Lubbock, TX 79409 USA. E-mail: Paul.pare@ttu.edu; Fax: +1 806 742 1289

Electronic Supplementary Information (ESI) available: [details of supplementary information available]. See DOI: 10.1039/x0xx00000x

ARTICLE

RSC Advances

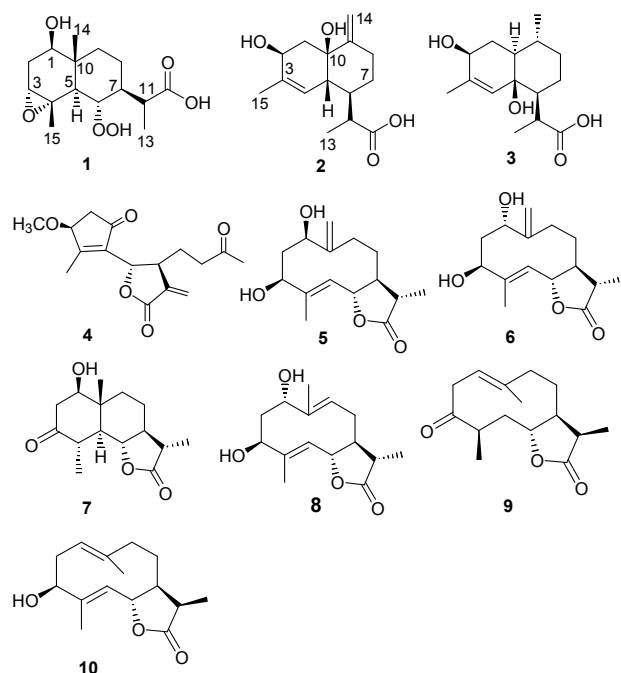


Figure 1. Isolated compounds from *Tanacetum sinaicum*.

presence of three methyl groups at δ_C 12.6, 21.3, and 25.5, four oxygenated signals at δ_C 57.6, 61.1, 64.2, and 81.0, three methylenes at δ_C 22.6, 31.7, and 33.9, three methines at δ_C 41.2, 50.4 and 51.2, and one carbonyl at δ_C 179.6 (Table 1). The most oxygenated down-field carbon signal indicated the presence of a

hydroperoxyl functionality confirmed by HRFABMS.¹⁸ From these data, four degrees of unsaturation were deduced suggesting a bicyclic sesquiterpene skeleton. Based on spectral correlations with previously identified **7**,¹⁵ the multiplet signal at δ_H 2.23 that correlated with methyl at δ_H 1.19 (3H, d, $J = 6.8$, H-13) and a methine at δ_H 1.56 (m, H-7) in DQF-COSY as well as δ_C 179.6 (C=O, C-12), 12.6 (q, C-13), 51.2 (d, C-7) and 81.0 (d, C-6) in HMBC allowing for the assignment of the multiplet signal to H-11. Based on HRFABMS and the carbon chemical shift (Table 1) the carbonyl at C-12 was assigned as a carboxylic acid group. Using H-7 as a starting point, DQF-COSY correlations allowed for assignments of δ_H 3.95 (t, $J = 11.0$, H-6), 1.71 (brd, $J = 13.0$, H-8a) / 1.29 (brq, $J = 12.4$, H-8b) and in turn 1.04 (td, $J = 14.4$, 4.7, H-9a) / 2.23 (m, H-9b) was identified from H-8. H-6 correlated with δ_H 1.80 (d, $J = 11.7$, H-5) and δ_C 22.6 (C-9), 38.9 (C-10), 50.4 (C-5), 51.2 (C-7), and 57.6 (C-4), in ^1H - ^1H COSY and HMBC analyses, respectively (Fig. 2). The downfield C-6 chemical shift was diagnostic for a hydroperoxyl functionality. HMBC correlation of H-5 with oxygenated signals at δ_C 57.6, 61.1, 64.2, and 81.0 and aliphatic signals at δ_C 38.9, and 33.9 allowed for the assignment of C-4, C-3, C-1, C-6, C-10, and C-9, respectively (Fig. 2). The upfield oxygenated C-3/C-4 chemical shifts were diagnostic for an epoxide functionality that was also consistent with HRFABMS data. HMBC correlations of δ_H 1.39 with C-3, C-4 and C-5 allowed for the methyl assignment of H₃-15. HMQC correlations with C-1 and C-3 established δ_H 3.69 (dd, H-1) and 3.12 (brs, H-3), respectively. The upfield signal at δ_C 64.2 was indicative of a hydroxyl functionality at C-1. DQF-COSY correlations were observed between H-1 and H-3 with δ_H 1.79 (t, $J = 13.1$, H-2b) / 2.40 (brdd, $J = 14.4$, 5.5, H-2a).

Table 1. NMR spectroscopic data for **1-3** with J in Hz (^1H NMR 600 MHz and ^{13}C 150 MHz, δ -ppm, CDCl_3).

No	1		2		3	
	δ_H	δ_C	δ_H	δ_C	δ_H	δ_C
1	3.69 dd (10.4, 5.5)	64.2 d	2.08 m *	35.9 t	1.75 m	30.9 t
			2.33 m *		1.97 m	
2	1.79 t (13.1)	31.7 t	3.96 d (5.5)	67.1 d	4.08 t (4.8)	67.2 d
	2.40 br dd (14.4, 5.5)					
3	3.12 br s	61.1 d	--	135.0 s	--	141.7 s
4	--	57.6 s	5.49 brs	123.3 d	5.35 s	129.0 d
5	1.80 d (11.7)	50.4 d	2.36 m*	40.6 d	--	84.2 s
6	3.95 t (11.0)	81.0 d	1.94 tt (11.7, 2.7)	43.9 d	1.95 m	46.7 d
7	1.56 m	51.2 d	1.27 m	26.5 t	1.47 m	22.3 d
			1.50 m		1.75 m	
8	1.29 br q (12.4)	22.6 t	2.10 m	32.6 t	1.24 m	25.5 t
	1.71 br d (13.0)		2.40 m		1.62 m	
9	1.04 td (14.4, 4.7)	33.9 t	--	148.0 s	1.95 m	29.0 t
	2.23 m		--			
10	--	38.9 s	--	86.0 s	2.08 m	38.5 d
11	2.23 m	41.2 d	2.85 m	39.9 d	2.54 m	40.8 d
12	--	179.6 s	--	181.3 s	--	179.5 s
13	1.19 d (6.8)	12.6 q	1.10 d (7.5)	9.6 q	1.05 d (7.5)	15.6 q
14	0.94 s	21.3 q	4.95 brs	109.6 t	0.93 d (7.0)	17.5 q
			5.28 brs			
15	1.39 s	25.5 q	1.85 s	20.8 q	1.83 s	20.5 q

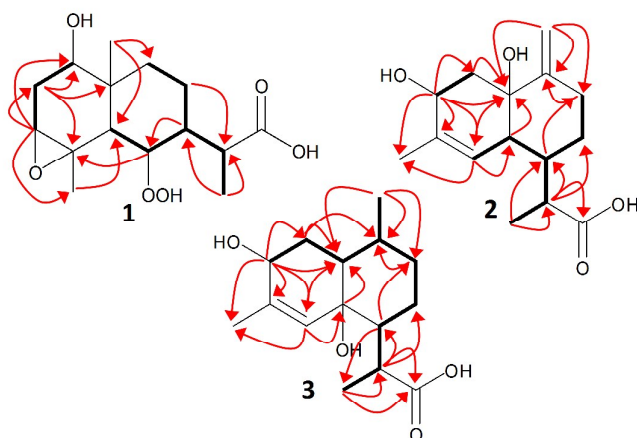


Figure 2. Selected ^1H - ^1H COSY (—) & HMBC (→) correlations of **1-3**.

HMBC correlations between H-1 and δ_{C} 21.3 allowing the assignment of H-14. Full NMR spectroscopic data assignments of **1** (Tables 1) were consistent with DQF-COSY, HMQC and HMBC data (Fig. 2). The relative stereochemistry assignment of H-7 to an α -configuration was based on biogenetic precedent and was consistent with previously reported NMR chemical shifts for similar sesquiterpene lactones.^{14,16} Relative stereochemistry at C-6 was based on a large coupling constant between H-7 and H-6 (11.0 Hz) indicating a *trans* configuration and the two protons in a α , β -*trans*-orientation. NOESY correlations between H-7, H-8a and H-5 indicated an α -configuration for these proton (Fig. 3) and a correlation between H-5 and H-1 indicated an α -configuration of H-1 and a β -orientation for the hydroxyl. Correlations between H-6 β /H₃-14 and H₃-14/H₃-15 indicated a β -orientation for H₃-14 and H₃-15 and an α -configuration for the epoxy group at C-3/C-4. Therefore the structure of **1** was assigned as 1 β -hydroxy,11methyl,3 α ,4 α -epoxy-6 α -hydroperoxy-eudesman-13-oic acid (tanacetolide A).

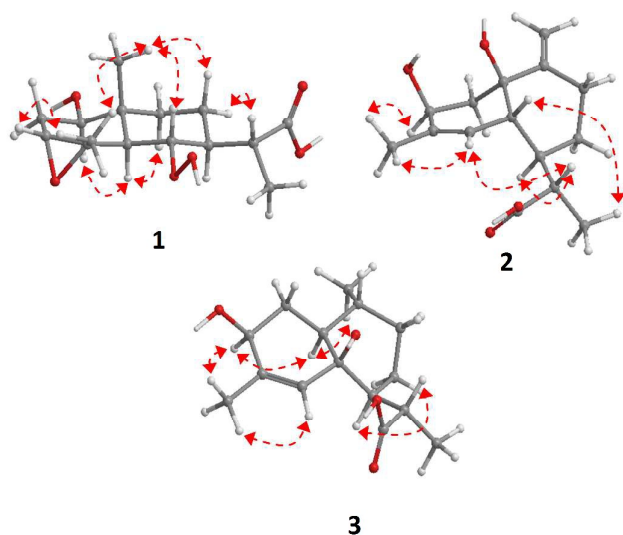


Figure 3. NOESY correlations for **1-3**.

Compound **2** was isolated as a colorless oil with an optical rotation of $[\alpha]_{\text{D}}^{25}$ -31.2 in MeOH. HRFABMS analysis showed a molecular ion peak at m/z 289.1425 $[\text{M}+\text{Na}]^+$ (calcd. for $\text{C}_{15}\text{H}_{22}\text{O}_4\text{Na}$, 289.1416), corresponding to the molecular formula $\text{C}_{15}\text{H}_{24}\text{O}_4$. The IR spectrum showed bands at 3450 cm^{-1} (OH), 1695 cm^{-1} (CO) and 3230 cm^{-1} (C=CH). In accordance with the molecular formula, 15 signals were resolved in the ^{13}C NMR spectrum (Table 1) and were further classified by DEPT to 2 methyls, 4 methylenes (1 olefinic), 5 methines (1 oxygenated, 1 olefinic), and 4 quaternary carbons (1 oxygenated, 1 keto and 2 olefinic). The ^1H NMR spectrum showed the appearance of two methyl groups at 1.85 (s) and 1.10 (d, $J = 7.5$), an oxygenated signal at δ_{H} 3.96 (d, $J = 5.5$) and broad singlets for exomethylene protons at δ_{H} 4.95 and 5.28 (Table 1). Five degrees of unsaturation were deduced, suggesting a bicyclic sesquiterpene skeleton. Two-dimensional COSY, HMQC and HMBC analyses (Fig. 2) and comparisons with published analogues indicated a 6/6 bicyclic cadinane-type sesquiterpene.¹⁹ The appearance of a downfield signal at δ_{C} 86.0 indicated an oxygenated functionality located in the fused ring system and δ_{H} 4.95 (brs) and 5.28 (brs) indicated an exomethylene functionality. Based on similar cadinane-type sesquiterpene structures, a characteristic olefinic H-4 was identified at δ_{H} 5.28 (brs)¹⁹ and using this as a point of reference, δ_{H} 2.36 (m), δ_{C} 135.0 (s), 20.8 (s), 43.9 (d), 67.1(d) and 86.0 (s) were identified as H-5, C-3, C-14, C-6, C-2, and C-10 respectively, by DQF-COSY and HMBC analyses (Fig. 2). ^{13}C NMR and DEPT analysis indicated that C-3 (δ_{C} 135.0) is a quaternary olefinic which was expected since an endocyclic double bond between C3/C-4 often is present with cadinane-type sesquiterpenes.^{19,20} The H-2 chemical shift established a hydroxyl at C-2^{19,20} and DQF-COSY allowed for the assignment of H₂-1 (δ_{H} 2.33/2.08, m). DQF-COSY analysis starting with H-5 also allowed for the assignment of H-6, H₂-7 and H₂-8. HMBC olefinic protons at δ_{H} 4.95 (brs) and 5.28 (brs) correlated with C-9 (δ_{C} 148.0), C-8 (δ_{C} 32.6) and C-10 (δ_{C} 86) indicating the location of the exomethylene double bond at C-9 and proton signal assignment to H₂-14. The downfield oxygenated carbon at δ_{C} 86.0 indicated a hydroxyl location being part of the quaternary fused-ring system that was assigned to C-10.²¹ The relative stereochemistry assignment for H 6 to an α -configuration was based on biogenetic precedent and was consistent with previously reported NMR chemical shift data for similar cadinane-type sesquiterpenes.¹⁹ H-6 NOESY correlations with δ_{H} 1.50 (m, H-7a) and 2.33 (m, H-1a) as well as between H-1a and H-2 indicated these protons to be on the same face in an α -configuration (Fig. 3). Additionally, H-5 correlated with δ_{H} 1.27 (m, H-7b) and 2.08 (m, H-1b) establishing that H-5 is on the opposite β -face. The β -orientation of the hydroxyl group at C-10 was assigned based on carbon shift data.^{20,21} Therefore **2** was assigned to 2 β ,10 β -dihydroxycadin-3,9(14)-dien-12-oic acid (tanacetolide B)

Compound **3** was isolated as a colorless oil with an optical rotation of $[\alpha]_{\text{D}}^{25}$ -41.6 in MeOH. HRFABMS analysis showed a molecular ion peak at m/z 291.1568 $[\text{M}+\text{Na}]^+$ (calcd. for $\text{C}_{15}\text{H}_{24}\text{O}_4\text{Na}$, 291.1572), corresponding to a molecular formula of $\text{C}_{15}\text{H}_{24}\text{O}_4$. IR bands were observed at 3450 cm^{-1} (OH), 1695 cm^{-1} (CO) and 3230 cm^{-1} (C=CH). Spectroscopic data were similar to **2** except the appearance of additional doublet for a methyl group at δ_{H} 0.93 (3H, $J = 7.0$) and the disappearance of exomethylene protons, suggesting

ARTICLE

RSC Advances

a substitution of the exomethylene group in **2** with a secondary methyl in **3**; this methyl substitution was confirmed by DEPT analysis. A correlation of δ_{H} 0.93 (3H, $J = 7.0$, H-14) with δ_{C} 38.5 (d) allowed for the assignment of H-10; a correlation of H-11 (1H, δ_{H} 2.54, m) with a downfielded quaternary oxygenated carbon signal at δ_{C} 84.2 confirmed the position of the hydroxyl group at C-5. ^1H - ^1H COSY, HSQC and HMBC spectroscopic data established the detailed structure. Compound **3** exhibited the same relative stereochemistry as **2** at C-2 and C-6. A NOESY correlation between H-2 and H-10/H-14 indicated that these protons are on the same α -face and that H-9 is on the opposite β -face (Fig. 3). The β -orientation of the hydroxyl group at C-5 was assigned based on carbon shift data.²² Therefore **3** was assigned to (2*S*,5*S*-dihydroxycadin-3-en-12-*o*-ic acid) (tanacetolide C).

To determine the inhibitory effect of the isolated compounds (**1-10**) in blocking NO production, an *in vitro* murine macrophage assay was performed using RAW264.7 cells. In these cells, lipopolysaccharide (LPS) alone induces iNOS transcription and protein expression as well as downstream NO production. This cell-based assay is used for drug screening of NO production inhibitors mediated by iNOS. Compound **4** inhibited NO production with an IC_{50} 1.0 μM which was even lower than the commercially available gold standard for NO inhibition, Caffeic acid phenethyl ester (CAPE) (Supplementary Table 1). Compound **1** exhibited intermediate inhibition with an IC_{50} of 15.7 μM , while other assayed compounds shown IC_{50} 's greater than 30 μM . To further investigate the mechanism of NO inhibition, iNOS protein expression was monitored in LPS-activated cells and lower iNOS protein levels were observed when cells were incubated with **4** (Fig. 4A). Since iNOS is MAPK regulated, protein levels for select MAPK protein components were examined. While LPS increased protein abundance for P-JNK, JNK, P-p38, P38, P-ERK and ERK, addition of **4** exhibited no change in protein abundance except at the highest 30 μM amount where protein levels for P-JNK, JNK, p38 and P-ERK were visually reduced (Fig. 4B). In contrast, p-IkBa protein levels that are induced with LPS are also inhibited by **4** in a dose-dependent manner (Fig. 4C). While **4** had no effect on protein

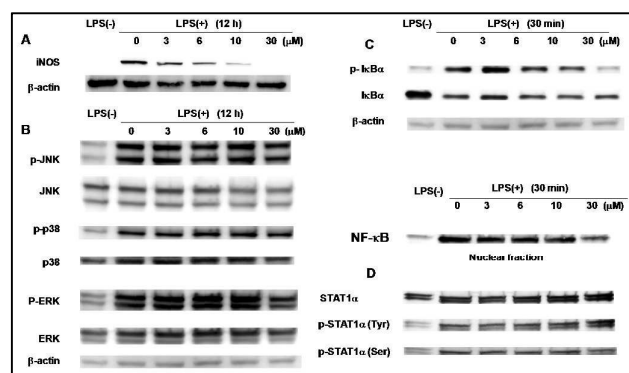


Figure 4. Western blot analysis of iNOS expression with and without the lipopolysaccharide activator (LPS) and with increasing amounts of **4** (0–30 μM) (A). Induction of signal transduction components including MAPK signaling (B), NF- κB (C) and STAT 1 (D) with **4** (0–30 μM). Cells were treated and cell lysates were prepared as described in the experimental section.

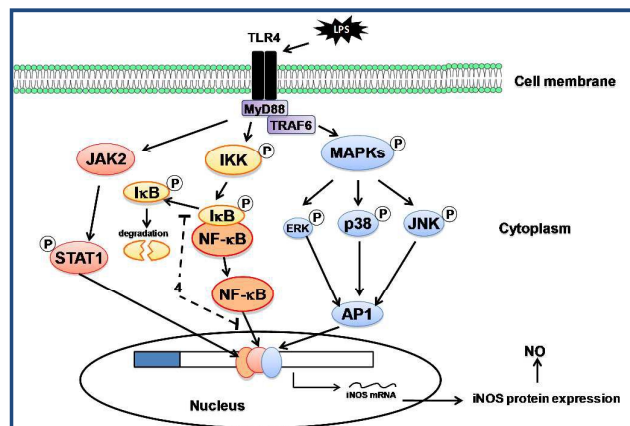


Figure 5. Inducible nitric oxide synthetase (iNOS) signaling pathway activated by lipopolysaccharide (LPS) binding the toll-like receptor 4 (TLR4) and transduced via mitogen-activated protein kinases MAPKs (ERK, p38 and JNK), the nuclear factor NF κB as well as a Janus tyrosine kinase (JAK) and signal transducers and activators of transcription (STATs). Other shown protein components that participate in iNOS signaling and are shown include: ERK (extracellular-regulated kinase), JNK (NH₂-terminal kinase), AP-1 (activating protein-1), MyD88 (myeloid differentiation primary response gene 88), IKK (I κB kinase) and I κB (NF κB inhibitor protein). Solid lines represent signaling connections for LPS-induced NO production. Treatment of RAW264.7 cells with **4** suppresses NF κB abundance in the nucleus (shown as a dashed line) thereby attenuating NF κB -mediated iNOS protein expression and downstream NO production.

abundance for STAT1 α , NF- κB translocation to the nucleus was inhibited (Fig. 4D), introducing the possibility that NF- κB inhibition may be a driver for iNOS protein expression. A model summarizing how **4** regulates NO production based on Western blot analysis is proposed (Fig. 5). A colorimetric assay using MTT for cytotoxicity indicated that **4** will need to be chemically modified before further studies to reduce cell toxicity levels ($\text{IC}_{50} = 4.3 \mu\text{M}$) (Suppl Fig. 1).

Experimental

General experimental procedures

Specific rotation was measured with a Horiba SEPA-300 digital polarimeter ($l = 5 \text{ cm}$) and IR spectra were collected on a Shimadzu FTIR-8100 spectrometer. For FAB-MS and HR-FAB-MS, a JEOL JMS-GCMATE mass spectrometer was used and ^1H (600 MHz) and ^{13}C (150 MHz) NMR spectra were recorded on a JEOL JNM-ECA 600 spectrometer with tetramethylsilane as an internal standard. Purification was run on a Shimadzu HPLC system equipped with a RID-10A refractive index detector and compound separation was performed on YMC-Pack ODS-A (250 x 4.6 mm i.d.) and (250 x 20 mm i.d.) columns for analytical and preparative separation, respectively.

Chromatography separation included normal-phase silica BW-200 (Fuji Silysia Chemical, Ltd., 150–350 mesh) and ODS reverse phase Chromatorex DM1020T (Fuji Silysia Chemical, Ltd., 100–200 mesh) columns as well as silica gel 60_{F254} (Merck, 0.25 mm) and RP-

18 WF_{254S} (Merck, 0.25 mm) TLC plates with spots developed with heating of H₂SO₄-MeOH (1:9) sprayed plates.

Plant Material

T. sinaicum (Fresen.) Delile ex was collected in June 2014 from North Sinia, Egypt and a voucher specimen SK-120 has been deposited in the herbarium of St. Katherine protectorate, Egypt.

Extraction and Isolation

Aerial parts (2.0 kg) were powdered and extracted with CH₂Cl₂-MeOH (1:1) at room temperature. The extract was concentrated *in vacuo* to obtain a residue of 160 g. The residue was fractionated on a silica gel column (6 x 120 cm) eluting with *n*-hexane (3 L) followed by a gradient of *n*-hexane-CHCl₃ up to 100 % CHCl₃ and CHCl₃-MeOH up to 50 % MeOH (3 L of each solvent mixture). The *n*-hexane-CHCl₃ (1:1) fraction was chromatographed on a Sephadex LH-20 column (3 x 90 cm) eluted with *n*-hexane-methylene chloride-methanol (7:4:0.25). Collected sub-fractions were re-chromatographed by RP HPLC using MeOH/H₂O (85-15%) to afford **2** (5 mg) and **9** (30 mg). The *n*-hexane-CHCl₃ (1:2) fraction was chromatographed on a Sephadex LH-20 column (3 x 90 cm) eluted with *n*-hexane-methylene chloride-methanol (7:4:0.25). Collected sub-fractions were further purified by RP HPLC using MeOH/H₂O (75-25%) to afford **3** (6 mg), and **10** (22 mg). The CHCl₃ (100%) fraction was chromatographed on a Sephadex LH-20 column (3 x 90 cm) eluted with *n*-hexane-methylene chloride-methanol (7:4:0.5). Collected sub-fractions were further purified by RP HPLC using MeOH/H₂O (65-35%) to afford **1** (15 mg), **4** (5 mg) and **7** (30 mg). The CHCl₃:MeOH (95:5) fraction was chromatographed on an ODS silica gel column (3 x 90 cm) eluted with MeOH:H₂O (70:30). Collected sub-fractions was further purified by RP HPLC using MeOH/H₂O (55-45%) to afford **5** (18 mg), **6** (17 mg) and **8** (15 mg).

Tanacetolide A (1) (1β-hydroxy,11methyl,3α,4α-epoxy-6α-hydroperoxy-eudesman-13-oic acid) Colorless oil [α]_D²⁵ = +55.6 (c 0.01, MeOH); for ¹H- (CDCl₃, 600 MHz) and ¹³C- (CDCl₃, 150 MHz) NMR, see Table 1. FABMS *m/z* 267 [M-OOH]⁺, HRFABMS *m/z* 267.1590 (calcd. for C₁₅H₂₃O₄: 267.1596); IR (ν_{\max} cm⁻¹) = 3450, 1695 cm⁻¹.

Tanacetolide B (2) (2β,10β-dihydroxycadin-3,9(14)-dien-12-oic acid) Colorless oil [α]_D²⁵ = -31.2 (c 0.01, MeOH); for ¹H- (CDCl₃, 600 MHz) and ¹³C- (CDCl₃, 150 MHz) NMR, see Table 1. FABMS *m/z* 289 [M+Na]⁺, HRFABMS *m/z* 289.1425 (calcd for C₁₅H₂₀O₅Na: 289.1416); IR (ν_{\max} cm⁻¹) = 3450, 3230, 1695 cm⁻¹.

Tanacetolide C (3) (2β,5β-dihydroxycadin-3-en-12-oic acid) Colorless oil [α]_D²⁵ = -41.6 (c 0.01, MeOH); for ¹H- (CDCl₃, 600 MHz) and ¹³C- (CDCl₃, 150 MHz) NMR, see Table 1. FABMS *m/z* 291 [M+Na]⁺, HRFABMS *m/z* 291.1568 (calcd for C₁₅H₂₀O₅Na: 291.1572); IR (ν_{\max} cm⁻¹) = 3450, 3230, 1695 cm⁻¹.

Bioassay Protocol

Murine macrophage cells (RAW264.7, ATCC No. TIB-71) were obtained from Dainippon Pharmaceutical, Osaka, Japan and cultured in Dulbecco's modified Eagle's medium (DMEM, high

glucose) supplemented with 5% fetal calf serum, penicillin (100 U/ml) and streptomycin (100 μg/ml) (Sigma Chemical Co., St. Louis, MO, USA). The cells were incubated at 37 °C in 5% CO₂/air.

NO Determination

For NO screening, cells were assayed as described previously (Sae-Wong et al., 2011). Briefly, cells were cultured in Dulbecco's Modified Eagle's Medium (DMEM), and cell suspensions were seeded into 96-well microplates at 2.5×10⁵ cells/100 μl/well. After 6 h, non-adherent cells were removed by washing with phosphate buffered saline (PBS) and adherent cells were cultured for 10 min in 100 μl of fresh medium containing one of the test compounds; LPS (10 μg/ml) isolated from *E. coli* (055: B5, Sigma) was used as to activate NO production. NO emissions was based on amount of nitrite consumed in the medium. Nitrite concentration was determined by a Griess reaction using a supernatant aliquot. Inhibition (%) was based on the formula shown and the IC₅₀ was determined graphically (*n*=4). Inhibition (%) = [(A-B)/(A-C)]×100
A-C: nitrite concentration (μg/ml); A: LPS (+), sample (-); B: LPS (+), sample (+); C: LPS (-), sample (-).

SDS-PAGE and Western Blot Analysis

For iNOS detection, cells (5.0×10⁶ cells/2ml/well) were seeded into a 6-well multiplate and allowed to adhere for 6 h at 37 °C in a humidified atmosphere containing 5% CO₂.²³ Cells were then washed with PBS and diluted with DMEM (1 ml) containing individual test compounds. After incubation (10 min), DMEM (1 ml) containing LPS (10 μg/ml) was added and incubated for 30 min or 12 hrs. The adhered cells were collected using a cell scraper in a lysis buffer [8.4 ml of distilled water, 100 μl of protease inhibitor cocktail (Thermo Scientific), 100 μl of 22% triton X-100, phosphatase inhibitor cocktail (PhosSTP, Roche), and 1 ml of a sample buffer (0.877 g NaCl, 0.121 g Tris, 0.612g β-glycerophate, 0.076 g EGTA, and 100 ml H₂O, pH 7.4)]. Cells were then disrupted three times (Microson™ ultrasonic cell disruptor, USA) for 30 s and centrifuged at 10,000 rpm for 10 min. Cell lysates protein concentrations were determined using a BCA™ protein assay kit. For protein sample preparation, 100 μl of supernatant was transferred to 100 μl of a dissolving agent (0.3423 g EGTA, 6 g SDS, 3.634 g Tris, 100 ml H₂O, 8 ml glycerol and 0.03 g bromophenol blue) and samples were heated in boiling water for 5 min. After cooling, samples were kept at -80°C until analysis.

The nuclear protein fraction was extracted for 30 min after LPS stimulation using a nuclear and cytoplasmic extraction reagent (Thermo Scientific), according to the manufacturer's instructions. The nuclear protein solution was concentrated using centrifugal filter units (Millipore Co., Ltd.) and protein separated by electrophoresis. Equivalent protein amounts (50 μg of protein/lane for iNOS and β-actin, 25 μg of protein/lane for proteins assayed) were run in 10% SDS-polyacrylamide gels (Bio-Rad ready gel J) and transferred onto polyvinylidene difluoride (PVDF) membranes (BioRad, NC, USA). The membrane was then soaked in tris-buffered saline containing 0.1% Tween 20 (T-TBS) with gentle shaking for 10 min (3X). For the blocking of the nonspecific sites, the membrane was soaked in blocking one-P (for phosphorylated proteins: p-ERK1/2, p-JNK, p-p38, p-STAT1, p-IkB; Nacalai Tesque, Japan) or

ARTICLE

RSC Advances

blocking one (for others: iNOS, ERK1/2, JNK, p38, NFκB, Iκβ and β-actin) by shaking for 0.5 h. The membrane was rinsed with T-TBS and incubated with specific primary antibodies: p-ERK1/2, ERK1/2, JNK1/2, p38, p-p38, NFκB p65, STAT1α, p-STAT1α (Ser), p-STAT1α (Tyr), p-IκB, iNOS and β-actin (1:1000, Cell Signaling Technology). After incubation for 1 hr at rt, the membrane was rinsed in T-TBS, and incubated secondary antibodies (HRP-conjugated goat anti-mouse and anti-rabbit IgG, 1:5000) in an immune-reaction enhancer solution (Can Get Signal, Toyobo, Japan) for 1 hr. The membrane was then shaken in T-TBS at 75 rpm for 10 min (3X). Proteins were detected using an enhanced chemiluminescence (ECL) plus Western blotting detection system (Amersham™ GE Healthcare, Biosciences). Membrane images were recorded using a luminescent image analyzer LAS-4000 mini (Fuji film, Japan).

Cytotoxic Determination

Cytotoxicity was evaluated by the 3-(4,5-dimethyl-2-thiazolyl)-2,5-diphenyl-2H-tetrazolium bromide (MTT) colorimetric assay according to a reported procedure²⁴ with slight modifications. Briefly, cells (1.0×10^5 cells/200 μl/well) were incubated with **4** (0-10 μM) for 18 h. An aliquot of the medium (100 μl) was removed and MTT solution (10 μl, 5 mg/ml in PBS) was added. After a 2-hr incubation at 37 C, the medium was removed and isopropanol containing 0.04 M HCl was added to dissolve the produced formazan. Optical density (OD) for the formazan solution was measured at 570 nm (reference: 655 nm). Percent viability compared to the solvent control (DMSO) was plotted against concentration and an IC₅₀ value was calculated using regression analysis.

Statistical analysis

All data are expressed as means ± S.E.M. Data analysis was performed with a one-way analysis of variance (1-ANOVA), followed by Dunnett's test. A *p*-value ≤ 0.05 was considered statistically significant. The IC₅₀ value was determined by regression analysis.

Conclusion

T. sinicum afforded new sesquiterpenes tanacetolide A-C (**1-3**) together with known compounds (**4-10**). Compound **4** inhibited NO production with an IC₅₀ of 1.0 μM, lower than the commercially available gold standard for NO inhibition, CAPE. Compound **4** exhibited no change in protein abundance for P-JNK, JNK, P-p38, P38, P-ERK and ERK except at the highest 30 μM amount where protein levels for P-JNK, JNK, p38 and P-ERK were slightly reduced.

Acknowledgements

This research was supported in part by National Research Center, Egypt, a postdoctoral fellowship from the Japan Society for the Promotion of Sciences (JSPS) (ID No. P10117) and the Welch Foundation (D-1478).

Notes and references

- 1 Triana, J. L. Eiroa, M. Morales, F. J. Pérez, I. Brouard, M. T. Marrero, S. Estévez, J. Quintana, F. Estévez, Q. A. Castillo, and F. León, *Phytochem.*, 2013, 92, 87-104.
- 2 M. J. Abad, P. Bermejo and A. Villar, *Phytotherapy Research.*, 2006, 9, 79-92.
- 3 W. C. Evans, D. Evans and W. B. Saunders, *Trease and Evans Pharmacognosy*, 2002, 15th Ed., Co. Ltd., London
- 4 T. G. Tutin, A. R. Clapham, and E. F. Warburg, *Excursion Flora of British Isles*. 1964, Cambridge Press, UK.
- 5 A. El-Shazly, G. Dorai, and M. Wink, *Z. Naturforsch.*, 2002, 57c, 620-623.
- 6 M. V. Cronauer, Y. Ince, R. Engers, L. Rinnab, W. Weidemann, C. V. Suschek, M. Burchardt, H. Kleinert, J. Wiedenmann, H. Sies, R. Ackermann and K. D. Kroncke, *Oncogene*, 2007, 26, 1875-1884.
- 7 C. Nathan, and Q. Xie, *J. Biol. Chem.* 1994, 269, 13725-13728.
- 8 C. Tan, A. Mui, and S. Dedhar, *J. Biol. Chem.*, 2002, 277, 3109-3116.
- 9 H. J. Kim, K. Tsoyi, J. M. Heo, Y. J. Kang, M. K. Park, Y. S. Lee, J. H. Lee, H. G. Seo, H. S. Yun-Choi, and K. C. Chang, *J. Pharmacol. Exp. Ther.*, 2007, 320, 782-789.
- 10 H. Y. Mina, S. H. Song, B. Lee, S. Kim, and S. K. Lee, *Chemistry & Biodiversity* 2010, 7, 409-414.
- 11 H. Matsuda, I. Toguchida, K. Ninomiya, T. Kageura, T. Morikawa, and M. Yoshikawa, *Bioorg. Med. Chem.*, 2003, 11, 709-715.
- 12 J. A. Marco, J. F. Sanz-Cervera, E. Manglano, F. Sancenon, A. Rustaiyan, and M. Kardar, *Phytochem.*, 1993, 34, 1561-1564.
- 13 M. Talzhanov, S. Raldugin, and A. Atazhanova, *Chem. Nat. Comp.* 2005, 41, 423-425.
- 14 A. Mahmoud, and T. Iinuma, *Phytochem.*, 1994, 36, 393-398.
- 15 J. A. Marco, J. F. Sanz-Cervera, V. Garcia-Lliso, J. Valles-Xirau, *Phytochem.* 1997, 44, 1133-1137.
- 16 M. Abdel-Mogib, J. Jakupovic, E. M. Dawidar, M. E. Metwally, M. Abou-Elzahab, *Phytochem.*, 1989, 28, 268-271.
- 17 M. Todorova, A. Trendafilova, B. Mikhova, A. Vitkova, and H. Duddeck, *Phytochem.*, 2007, 68, 1722-1730.
- 18 A. Rustaiyan, and S. Famarzi, *Phytochem.*, 1988, 27, 479-481.
- 19 Z.-M. Feng, S. Song, P.-F. Xia, J.-S. Jiang, and P.-C. Zhang, *Helvetica Chimica Acta*, 2009, 92, 1823-1828.
- 20 S. A. Elmarakby, F. S. El-Ferally, H. N. Elsohaly, E. M. Croom, and C. D. Hufford, *Phytochem.*, 1988, 27, 3089-3091.
- 21 J. Zhou, J. S. Wang, Y. Zhang, P. R. Wang, C. Guo, and L. Y. Kong, *Chem. Pharm. Bull.*, 2012, 60, 1067-1071.
- 22 G. Fontana, S. La Rocca, S. Passannanti, and M. P. Paternostro, *Nat Prod Res.*, 2007, 21, 824-827.
- 23 C. Sae-Wong, H. Matsuda, S. Tewtrakul, P. Tansakul, S. Nakamura, Y. Nomura, and M. Yoshikawa, *J. Ethnopharmacol.* 2011, 136, 488-495.